

# BRUECKNER THEORY OF NUCLEAR MATTER WITH NONNUCLEONIC DEGREES OF FREEDOM AND RELATIVITY <sup>\*†</sup>

R. MACHLEIDT

*Department of Physics, University of Idaho, Moscow, ID 83844, USA*

*E-mail: machleid@uidaho.edu*

For the past 40 years, Brueckner theory has proven to be a most powerful tool to investigate systematically models for nuclear matter. I will give an overview of the work done on nuclear matter theory, starting with the simplest model and proceeding step by step to more sophisticated models by extending the degrees of freedom and including relativity. The final results of a comprehensive hadronic theory of nuclear matter are compared to the predictions by currently fashionable two-nucleon force models. It turns out that a two-nucleon force can, indeed, reproduce those results *if the potential is nonlocal*, since nonlocality is an inherent quality of the more fundamental fieldtheoretic approach. This nonlocality is crucial for creating sufficient nuclear binding.

## 1 Introduction

By definition, *nuclear matter* refers to an infinite uniform system of nucleons interacting via the strong force without electromagnetic interactions. This hypothetical system is supposed to approximate conditions in the interior of a heavy nucleus. We shall assume equal neutron and proton densities; that is, we will consider symmetric nuclear matter. This many-body system is characterized by its energy per nucleon as a function of the particle density. Based upon various semi-empirical sources, nuclear matter is determined to saturate at a density  $\rho_0 = 0.17 \pm 0.02 \text{ fm}^{-3}$  (equivalent to a Fermi momentum  $k_F = 1.35 \pm 0.05 \text{ fm}^{-1}$ ) and an energy per nucleon  $\mathcal{E}/A = -16 \pm 1 \text{ MeV}$ .

Historically, the first nuclear matter calculations were performed by Heisenberg's student Hans Euler, in 1937.<sup>1</sup> This was just two years after Weizäcker<sup>2</sup> had suggested the semiempirical mass formula. Euler applied an attractive potential of Gaussian shape in second-order perturbation theory.

Modern studies began in the early 1950's after a repulsive core in the nuclear potential had been conjectured.<sup>3</sup> It was obvious that conventional perturbation theory was inadequate to handle such singular potentials. Therefore, special methods had to be developed. This program was initiated by *Keith Brueckner* and co-workers<sup>4,5,6</sup> who applied—for the ground-state problem of nuclei—methods similar to those developed by Watson<sup>7</sup> for multiple scattering. Later, a formal basis for this new approach was provided by Goldstone<sup>8</sup> who, using perturbation theoretical methods, established the so-called linked cluster expansion. The success of Brueckner theory in practical calculations stems from the fact that certain classes of linked diagrams can be summed in closed form up to infinite orders defining the so-called

---

<sup>\*</sup>INVITED TALK PRESENTED AT THE *TENTH INTERNATIONAL CONFERENCE ON RECENT PROGRESS IN MANY-BODY THEORIES*, SEPTEMBER 10–15, 1999, SEATTLE, WASHINGTON, USA; TO BE PUBLISHED IN *ADVANCES IN QUANTUM MANY-BODY THEORY*, VOL. 3 (WORLD SCIENTIFIC, SINGAPORE).

<sup>†</sup>DEDICATED TO KEITH BRUECKNER ON THE OCCASION OF HIS 75TH BIRTHDAY.

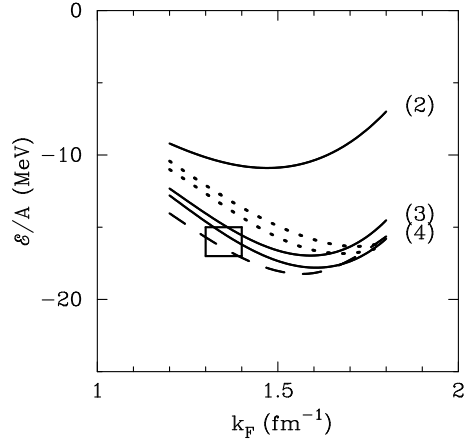


Figure 1. Energy per nucleon in nuclear matter,  $\mathcal{E}/A$ , versus the Fermi momentum,  $k_F$ , applying the Argonne  $V_{14}$  potential. Solid curves represent Brueckner results, using the gap choice for the single particle potential, with the number of hole lines indicated in parentheses. The dashed curve is the Brueckner two hole-line result using the continuous choice. The two dotted lines are obtained in variational calculations. The box describes the area in which nuclear saturation is expected to occur empirically. (Dashed curve from Ref. <sup>30</sup>, all other curves from Ref. <sup>26</sup>.)

reaction matrix  $G$ . All quantities are then formulated in terms of this  $G$  which—in contrast to the bare nuclear potential—is smooth and well behaved.

The first numerical calculations applying Brueckner theory were performed in 1958 by Brueckner and Gammel<sup>9</sup> using the Gammel-Thaler potential.<sup>10</sup> In the 1960s, Hans Bethe and his students elaborated thoroughly on Brueckner theory.<sup>11,12,13,14</sup> Around 1970, elegant numerical methods<sup>15,16</sup> for the solution of the Brueckner equation were established and systematic calculations performed.<sup>17,18</sup>

In the mid 1970s, the nuclear many-body community was shaken by an apparent discrepancy between results from Brueckner theory and the variational approach (the famous/infamous ‘nuclear matter crisis’<sup>19</sup>). This indicated that both many-body theories had to be reexamined and more consistent calculations had to be performed. For Brueckner theory, the necessary work was done mainly by Ben Day.<sup>20,21</sup> The variational approach was pursued by the Urbana group,<sup>22</sup> the Rome-Pisa collaboration,<sup>23</sup> and many others.<sup>24</sup> As a result of this enormous work, quantitatively very close predictions were finally obtained from the two different many-body approaches using realistic  $NN$  potentials.<sup>25,26,27</sup> Based upon these comprehensive investigations, it is now commonly accepted that both many-body approaches are reliable for densities typical for conventional nuclear physics.

Brueckner theory does not converge in powers of  $G$ , but in terms of the hole-line expansion.<sup>13</sup> This is demonstrated in Fig. 1 for the case of the Argonne  $V_{14}$  potential.<sup>28</sup> The solid lines in this figure are obtained from Brueckner theory using the conventional choice (‘gap choice’)<sup>29</sup> for the single particle potential; the number of hole lines taken into account are indicated in parentheses. The Brueckner results shown in Fig. 1 are from Day;<sup>26</sup> they were recently confirmed by Baldo

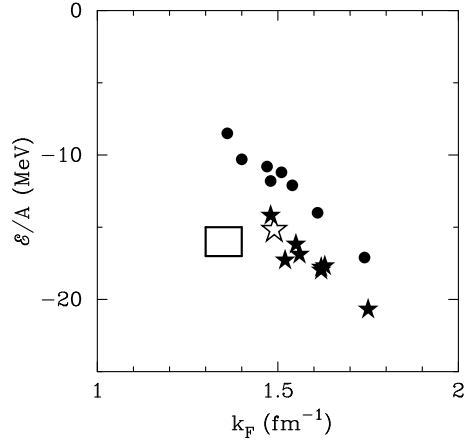


Figure 2. Nuclear matter saturation as predicted by a variety of  $NN$  potentials. Solid dots are the saturation points (i. e., minima of  $\mathcal{E}/A$  versus  $k_F$  curves) obtained in the Brueckner two hole-line approximation applying the gap choice for the single particle potential. Solid stars denote corresponding predictions that either include four hole-lines using the gap choice or two hole-lines using the continuous choice. The open star is the result by Brueckner and Gammel of 1958.<sup>9</sup>

and coworkers.<sup>30</sup> The dotted lines in Fig. 1 are the predictions by two variational calculations performed by Wiringa.<sup>26</sup> Within the uncertainties there appears to be agreement between Brueckner theory and the variational approach; particularly, around the minimum of the curves. Finally, the dashed curve in Fig. 1 is the lowest order Brueckner (i.e., two hole-line) result when the continuous choice<sup>29</sup> is used for the single particle potential.<sup>30</sup> It is clearly seen that this latter result agrees well with the four hole-line Brueckner prediction using the gap choice. This may suggest that the continuous choice is a more efficient way to perform Brueckner calculations.<sup>30,31,32,33</sup>

Systematic Brueckner calculations conducted with a variety of  $NN$  potentials show the so-called Coester Band<sup>17</sup> structure (Fig. 2): no prediction is able to reproduce the empirical saturation density *and* energy simultaneously. If the density is predicted right the energy is too high, and if the energy is right the density is too high. The predictions discussed so far were obtained in the framework of the simplest model for the atomic nucleus: point nucleons obeying the nonrelativistic Schrödinger equation interact through a static two-body potential that fits low-energy  $NN$  scattering data and the properties of the deuteron. This conventional model for the nucleus is obviously insufficient to quantitatively describe the nuclear ground state. It is, therefore, necessary to go beyond the conventional scheme.

To get some structure into the upcoming considerations, we list in Table 1 four items relevant to the nuclear many-body problem. The assumptions made in the conventional approach are given in column two. Column three states some obvious ideas leading beyond the conventional model. Notice that the distinction between the various items and assumption is artificial and that there is a great deal of overlap among them. Step by step, we will now include most of the possible

Table 1. **Basic assumptions underlying the nuclear many-body problem**

<i>Item</i>	<i>Simplest assumption</i>	<i>Possible extension(s)</i>
<b>Degrees of freedom</b>	Nucleons only	Mesons, Isobars, Quarks and gluons
<b>Hadron structure</b>	Point structure	(Quark) sub-structure
<b>Interaction(s)</b>	Static, instantaneous two-body potential	Non-static interactions, Many-body forces
<b>Dynamical equation</b>	Non-relativistic Schrödinger equation	Relativistic Dirac equation

extensions in nuclear matter calculations. One great advantage of Brueckner theory is that it allows to take into account additional degrees of freedom in a fairly easy and straightforward way.

## 2 Meson Degrees of Freedom

Ever since the meson hypothesis was formulated, it was (at least in principal) clear that the full nuclear many-body problem should include nucleons *and* mesons. Nevertheless, traditionally only nucleons have been considered, these interacting via a static two-body potential. Even in cases where the two-nucleon force was derived from meson theory, the mesons were usually “forgotten” as soon as the nuclear force was constructed. “Meson theory” was merely used to provide a suitable ansatz for the two-body potential with a convenient parametrization in terms of masses and coupling parameters. Thus, the dynamical presence of the mesons was ignored. Obviously, from a more fundamental point of view, this is not satisfactory.

Therefore, we will now include meson degrees of freedom in Brueckner theory following the approach suggested by Schütte.<sup>34</sup> This approach is fieldtheoretic in nature, treating baryons and mesons *a priori* on an equal footing. However, a principal problem of every field-theoretic many-body theory is how to take into account the effects of the many-body environment on the particles and their interactions (e. g. the single-particle energies in the medium, propagation in the medium, etc.). This is difficult to do in a covariant way. Therefore, Schütte suggested to use time-ordered (“old-fashioned”) perturbation theory,<sup>35</sup> which is similar to the usual perturbation theory of ordinary quantum mechanics. Thus, methods familiar from non-relativistic many-body theories can be used.

Starting from a field-theoretic Hamiltonian for mesons and nucleons

$$h = t + W, \quad (1)$$

where  $t$  denotes the unperturbed Hamiltonian (i. e., the operator for the free rela-

tivistic energies of nucleons,  $E_m = \sqrt{M^2 + \mathbf{q}_m^2}$ , and mesons,  $\omega_\alpha = \sqrt{m_\alpha^2 + \mathbf{k}_\alpha^2}$ ) and  $W$  the meson-nucleon interactions, and applying time-ordered perturbation theory, the lowest order contribution to free-space two-nucleon scattering is of second order, namely,

$$V(z) = W \frac{1}{z - t + i\epsilon} W, \quad (2)$$

with  $z$  the relativistic free energy of the two interacting nucleons (i. e.,  $z = E_m + E_n$  for nucleon  $m$  and  $n$ ). Equation (2) can be understood as an one-boson-exchange (OBE) “quasi-potential” (which is energy dependent). The Lippmann-Schwinger equation for free-space two-nucleon scattering is

$$T(z) = V(z) + V(z) \frac{1}{z - t + i\epsilon} T(z). \quad (3)$$

Turning to the nuclear many-body problem, we introduce the single-particle potential  $U$  and rewrite the Hamiltonian Eq. (1) by

$$h = h_0 + h_1 \quad (4)$$

with the unperturbed Hamiltonian

$$h_0 = t + U \quad (5)$$

and the perturbation

$$h_1 = W - U. \quad (6)$$

As a consequence of this, the one-boson exchange, Eq. (2), is modified in the nuclear medium where it reads

$$\bar{V}(\bar{z}) = W \frac{1}{\bar{z} - h_0} W. \quad (7)$$

Similar to conventional Brueckner theory, the equation for the Brueckner  $G$  matrix is

$$\bar{G}(\bar{z}) = \bar{V}(\bar{z}) + \bar{V}(\bar{z}) \frac{Q}{\bar{z} - h_0} \bar{G}(\bar{z}). \quad (8)$$

This equation differs from the (free-space) Lippman-Schwinger equation (3) by the Pauli projector  $Q$  which projects onto unoccupied two-nucleon states (giving rise to the Pauli effect) and by the energy denominator  $[\bar{z} - h_0]$  which replaces  $[z - t + i\epsilon]$  of Eq. (3) (causing the dispersion effect). Both these effects are the crucial saturation mechanisms of conventional Brueckner theory. Note that in all results presented in this paper the conventional Brueckner effects are always included. In lowest order, the energy per nucleon in nuclear matter is given by

$$\frac{\mathcal{E}}{A} = \frac{1}{A} \sum_{m \leq k_F} E_m + \frac{1}{2A} \sum_{m, n \leq k_F} \langle mn | \bar{G}(\bar{z}) | mn - nm \rangle - M \quad (9)$$

with  $M$  the mass of the free nucleon. The single particle potential used in these calculations is defined by

$$U(m) = Re \sum_{n \leq k_F} \langle mn | \bar{G}(\bar{z}) | mn - nm \rangle \quad (10)$$

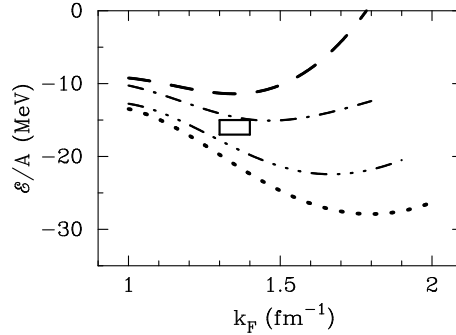


Figure 3. Results from nuclear matter Brueckner calculations that include medium effects on the two-nucleon interaction. The dotted line is obtained without such medium effects; the dash-triple-dot curve includes the medium effect on meson propagation; in addition to this, the dash-dot curve contains the dispersion effect from diagrams with intermediate  $\Delta$  states. Finally, the dashed curve includes all medium effects (i. e., also the Pauli effects from  $N\Delta$  intermediate states). All calculations are conducted in the two hole-line approximation using the continuous choice.

which is applied for nucleons below and above the Fermi surface (continuous choice). In the nuclear medium,

$$\bar{z} = \epsilon_m + \epsilon_n, \quad (11)$$

with

$$\epsilon_m = E_m + U_m, \quad (12)$$

in accordance with the unperturbed Hamiltonian  $h_0$ .

Formally, Eqs. (8)–(10) are essentially identical to ordinary Brueckner theory. The difference is in the quasipotential  $\bar{V}$  which depends on the nuclear medium (and its density). The impact of this medium effect is demonstrated in Fig. 3 where the dash-triple-dot curve is calculated with this effect while the dotted curve is without it. It is seen that the medium effect on meson propagation is such that the binding energy per nucleon is slightly reduced (in the order of 2 MeV at nuclear matter density). This effect is similar to the dispersion effect of ordinary Brueckner theory, but, much smaller. The density-dependence of this mesonic effect is such that the saturation point moves along the Coester band and not off it.

### 3 Isobar Degrees of Freedom

The excited states of the nucleon play an important role in a genuine and realistic meson-exchange model for the nuclear force. The lowest-lying pion-nucleon resonance, the  $\Delta(1232)$  isobar, is essential for  $NN$  scattering at low and intermediate energies. It provides a large part of the intermediate range attraction and it generates most of the inelasticity above pion-production threshold. Again, being aware of how crucial this degree of freedom is for the two-body interaction, we should not “freeze it out” in the many-body problem.

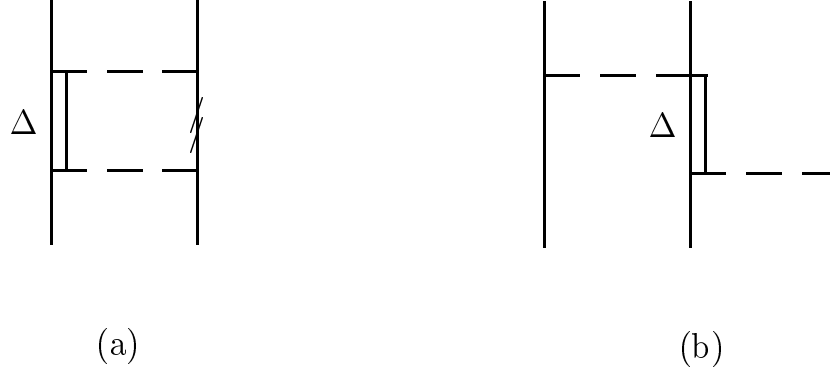


Figure 4. Two- and three-body forces created by the  $\Delta$  isobar. Solid lines represent nucleons, double lines  $\Delta$  isobars, and dashed lines  $\pi$  and  $\rho$  exchange. **Part (a)** is a contribution to the two-nucleon force. The double slash on the intermediate nucleon line is to indicate the medium modifications (Pauli blocking and dispersion effects) that occur when this diagram is inserted into a nuclear many-body environment. **Part (b)** is a three-nucleon force (3NF).

The lowest order in which isobars can contribute to the  $NN$  interaction is the fourth order in the interaction Hamiltonian  $W$  (which corresponds to a two-meson exchange). The general structure of the fourth order perturbation is for the case of free scattering

$$V^{(4)}(z) = W \frac{1}{z-t+i\epsilon} W \frac{1}{z-t+i\epsilon} W \frac{1}{z-t+i\epsilon} W \quad (13)$$

with  $W$  the meson baryon interaction. The irreducible part of these diagrams contributes to the “kernel”  $V(z)$  of the scattering equation. One of the diagrams generated by Eq. (13) is shown in Fig. 4(a). When inserted into the many-body problem the contribution  $V^{(4)}(z)$  is altered in a characteristic way; namely it is replaced by

$$\bar{V}^{(4)}(\bar{z}) = W \frac{Q}{\bar{z}-h_0} W \frac{Q}{\bar{z}-h_0} W \frac{Q}{\bar{z}-h_0} W \quad (14)$$

where the Pauli operator  $Q$  projects nucleons onto unoccupied nucleon states.

One can distinguish between two ways in which the medium exercises influence:

- The Pauli projector  $Q$  cuts out the lower part of the nucleon spectrum in intermediate states; this leads to the so-called *Pauli effect*.
- The propagator  $[z-t+i\epsilon]^{-1}$  is replaced by  $[\bar{z}-h_0]^{-1}$ ; the effect caused by this replacement has become known as *dispersion effect*.

Both effects reduce the absolute size of the diagram. Thus, for an attractive diagram there is a net repulsive medium effect. Notice that these two effects are similar to the conventional Brueckner effects discussed below Eq. (8).

Figure 3 includes the results employing the field-theoretic model just sketched. The inclusion of the dispersive effects under consideration moves us from the dash-triple-dot curve to the dash-dot curve, and the Pauli effects bring us further up to the dashed curve. This group of medium effects are substantially larger than those from the OBE terms discussed in the previous section.

The results presented in Fig. 3 are based upon the Bonn Full Model for the  $NN$  interaction.<sup>36</sup> This model includes also the (repulsive)  $\pi\rho$  diagrams (for which the medium effect causes a net attraction). However, since the sum of  $2\pi$  and  $\pi\rho$  diagrams is attractive, the  $2\pi$ -exchange being dominant at intermediate range, the net medium effect is repulsive. It is clearly seen that dispersion and Pauli effects are about equally important, the latter typically increasing more strongly with density. We note that these calculations also include all non-iterative diagrams (stretched and crossed box diagrams) involving  $\Delta$  isobars which contribute about as much to the medium effects as the box (iterative) diagrams.

The density-dependence of the effects due to  $\Delta$  degrees of freedom is only slightly stronger than that of the conventional saturation mechanisms, bringing the saturation point not markedly off the Coester band.

#### 4 Many-Body Forces

When discussing many-body forces, caution is in place. Notice that the diagram Fig. 4(b) is a genuine three-body force in a model space which consists of nucleon states only. In an extended Hilbert space which includes  $\Delta$  isobar states, Fig. 4(b) represents just a three-particle correlation. Thus, most many-body forces are artificially created by freezing out degrees of freedom. In this respect they are merely artefacts of the particular theoretical framework applied. Because of this model dependence of the terminology, it is useful to introduce an operating definition for *n-nucleon forces* which we will take to be the following: forces that depend in an irreducible way on the coordinates or momenta of *n nucleons* when *only nucleon degrees of freedom* are taken into account.

The fact that most many-body forces are an artifact of theory implies the following rule for how to deal with the many-body-force issue in a proper way: when you introduce a new degree of freedom, take it into account in the *two- and many-body problem*, consistently. Field-theoretic models for the  $2\pi$ -exchange contribution to the  $NN$  interaction require the  $\Delta(1232)$  isobar, which also creates *n-nucleon forces* in the many-body system. Consequently, when introducing the isobar degree of freedom, it should be included in the two- and many-nucleon forces simultaneously. In Fig. 4(a) we showed a contribution to the two-nucleon interaction that involves a  $\Delta$  isobar in the intermediate state; the existence of the  $\Delta$  isobar implies that, in the many-body system, the diagram Fig. 4(b) will occur (and many other diagrams involving  $\Delta$ s) which—according to the above definition—represents a three-nucleon force (3NF).

For a spin- or isospin saturated system, the lowest order term, Fig. 4(b), vanishes. However, when a third interaction between the nucleon legs is introduced, then there is a significant attractive contribution. A very thorough calculation of diagrams of this kind has been conducted by Dickhoff, Faessler, and Mütter.<sup>37</sup>



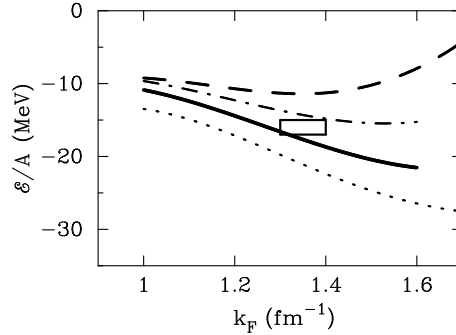


Figure 5. Many-nucleon force contributions to the nuclear matter energy. The dashed line is identical to the dashed line of Fig. 3. Adding the 3rd and 4th order ring diagrams with  $\Delta$ -isobars results in the dash-dot curve. The latter contributions are from the Tübingen group<sup>37</sup> who produced results for  $k_F \leq 1.6 \text{ fm}^{-1}$  only. Further contributions from meson and nucleon renormalization lead to the solid curve which is our final result. The dotted curve is identical to the dotted curve of Fig. 3 and includes neither medium effects on the two-nucleon force nor many-nucleon force contributions.

Speaking in terms of the hole-line expansion, these authors have calculated the three and four hole-line contributions of the ring type with isobar degrees of freedom. In terms of the ‘nucleons only’ language, the ring diagrams involving isobars are contributions from many-nucleon forces. The results obtained by the Tübingen group<sup>37</sup> are shown in Fig. 5.

The top line (dashed) in Fig. 5, which is the starting point of our quantitative considerations in this section, repeats the final result of the previous section; it is obtained in lowest order Brueckner theory (two hole-line approximation) and includes all medium effects on the two-nucleon interaction discussed in Sects. 2 and 3. Now, we add the attractive contributions from ring diagrams of third and fourth order involving  $\Delta$  isobars (i. e., 3NF and 4NF contributions) and arrive at the dash-dot curve in Fig. 5.

Another class of diagrams that belongs into the category of many-nucleon forces (according to the above definition) was calculated in Ref. <sup>38</sup> where it was shown that the selfenergy diagrams of  $\pi$  and  $\rho$  together with nucleon selfenergy corrections result in a net attractive effect (which in terms of magnitude is of the same size as the repulsive mesonic effect discussed in Sect. 2). When we add this contribution to the dash-dot curve in Fig. 5, then we obtain the solid curve which is our final result. In this figure, we also show again the dotted curve of Fig. 3 which represents the result when no medium effects and no many-nucleon forces were included. The comparison of the dotted curve with the solid curve in Fig. 5 reveals that the sum of all medium effects on the  $NN$  force plus all many-nucleon force contributions is much smaller than the individual contributions; or in other words, there are large cancelations. However, the cancelations are not perfect and the net effect is moderately repulsive.

To summarize this and the previous section, isobar degrees of freedom have essentially *two* consequences in nuclear matter:

- *medium effects* on the two-nucleon interaction and
- *many-nucleon force* contributions.

Both are *large effects/contributions* — but, of *opposite* sign. In a consistent treatment of degree(s) of freedom either both effects occur simultaneously, or none. One of these two effects alone, in isolation, does not exist in reality. Therefore, to take into account only one of them (for instance, only the three-body force contributions, ignoring the medium effects on the corresponding two-body diagrams) yields a substantially distorted picture. In fact, the almost cancelation between these two effects/contributions may be the deeper reason why, ultimately, many-body forces may not play a great role in nuclear physics; it may also be the reason why the traditional two-body force picture is by and large rather successful.

We note that our findings in nuclear matter are supported by accurate and independent calculations conducted for the triton binding energy. Triton calculations of this kind were first performed by the Hannover group.<sup>39</sup> Recently, these calculations have been improved and extended by Picklesimer and coworkers<sup>40</sup> using the Argonne  $V_{28}$   $\Delta$ -model.<sup>28</sup> They find an attractive contribution to the triton energy of  $-0.66$  MeV from the 3NF diagrams created by the  $\Delta$ , and a repulsive contribution of  $+1.08$  MeV from the dispersive effect on the two-nucleon force involving  $\Delta$  isobars. The total result is *0.42 MeV repulsion*.<sup>40</sup> This means that—also in the triton—the final result is a moderate repulsion, similar to our findings in nuclear matter. The consistency of the results for the two very different many-nucleon systems suggests that there may be some general validity and model-independence to our findings.

Besides the  $\Delta$ -isobar, there are other mechanisms that can give rise to three-nucleon forces. In recent years, it has become fashionable to consider chiral Lagrangians for nuclear interactions. Such Lagrangians may create diagrams which represent effective three-nucleon potentials. However, Weinberg has shown that all these diagrams cancel.<sup>41</sup> Moreover, based upon power counting arguments, one can show that chiral  $n$ -nucleon forces with  $n \geq 4$  are negligible.<sup>42</sup>

## 5 Comparison to Simple Models

In Sections 2 to 4, we have presented the results of the most comprehensive and consistent nuclear matter Brueckner calculations ever conducted in terms of hadronic degrees of freedom—with the final result given by the solid curve in Fig. 5. After all this work which took the research groups involved about a decade, one may raise a very naive, but reasonable question: how does this final result compare with the predictions from the usual simplistic approach in which a static (energy-independent) two-nucleon potential is applied?

To answer this question, we show in Fig. 6 the saturation curves generated by some  $NN$  potentials together with the ‘final result’ of Sect. 4 (thick solid curve, identical to solid curve of Fig. 5; note also that Figs. 5 and 6 have slightly different scales). The  $NN$  potentials applied in Fig. 6 are all from the new family of high-precision/high-quality potentials developed in the 1990’s.<sup>43,44,45</sup> These new potentials fit the  $NN$  data below 350 MeV laboratory energy with the ‘perfect’

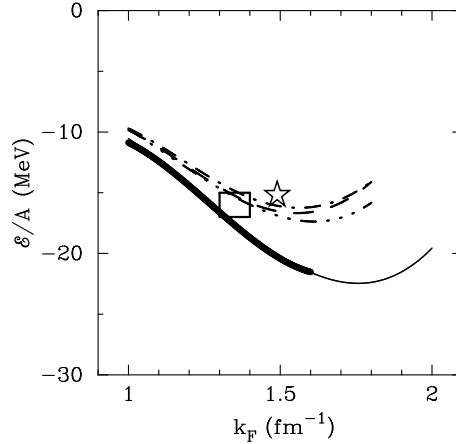


Figure 6. Nuclear matter predictions by some recent two-nucleon potentials. The dashed, dash-dot, and dash-triple-dot curves are produced by the (local) Argonne  $V_{18}$ ,<sup>44</sup> Nijm-II,<sup>43</sup> and Reid93<sup>43</sup> potentials, respectively; and the thin solid line is predicted by the (nonlocal) CD-Bonn<sup>45</sup> potential. The thick solid curve is identical to the solid curve of Fig. 5 and is shown for comparison. Note that this curve is given only for  $k_F \leq 1.6 \text{ fm}^{-1}$ , where it cannot be distinguished from the CD-Bonn curve on the scale of the figure. The star is the saturation point predicted by Brueckner and Gammel<sup>9</sup> in 1958. All calculations are based upon the two hole-line approximation using the continuous choice.

$\chi^2/\text{datum} \approx 1$ ; consequently, all these new potentials produce essentially identical predictions for the two-nucleon observables. However, this does not imply that these potentials are identical. Indeed, they differ in their off-shell behavior as indicated by the fact that some of these potentials are local and some nonlocal.

The Argonne  $V_{18}$ ,<sup>44</sup> Nijm-II,<sup>43</sup> and Reid93<sup>43</sup> potentials are local and their nuclear matter predictions are represented in Fig. 6 by the dashed, dash-dot, and dash-triple-dot curves, respectively. The CD-Bonn potential<sup>45</sup> is nonlocal and predicts the thin solid curve.

Figure 6 clearly reveals that all local potentials lead to almost identical nuclear matter results. This statement is even true if one includes the result by Brueckner and Gammel of 1958 with the local Gammel-Thaler potential (see star in Fig. 6). So, in terms of local potentials, there has not been much progress in the past 40 years.

The story is different with the nonlocal CD-Bonn potential which predicts a distinctly different result. Moreover, the nonlocal CD-Bonn reproduces amazingly well<sup>46</sup> the final result from the thorough and comprehensive calculations of Sects. 2 to 4.

Thus, the bottom line is that the result of the ‘faithful’ calculation that takes meson, nucleon and  $\Delta$  degrees of freedom consistently into account can, indeed, be reproduced by a two-nucleon potential. However, not by any potential, it has to be a nonlocal one. Or in other words, the nonlocality, which is one important element of the comprehensive theory of Sects. 2 to 4, cannot be ignored.

Since the CD-Bonn is based upon relativistic meson exchange, it contains the

same nonlocalities as the fieldtheoretic models applied in Sects. 2 to 4, except for the energy-dependence. This energy-dependence of the  $NN$  interaction can obviously be neglected—the reason being the large cancelations between the medium effects on the two-nucleon interaction (which are caused by the energy-dependence) and the  $n$ -nucleon force contributions. However, the other forms of nonlocality cannot be neglected. In short: you can make it simple but not too simple.

## 6 Relativistic ‘Dirac’ Effects

We will now explore an important effect not included in the systematic investigations conducted up to Sect. 4. Notice that, in the fieldtheoretic approach sketched in Sect. 2, one can go one step further and use the Dirac equation for single-particle motion in nuclear matter

$$(\not{p} - M - U)\tilde{u}(\mathbf{p}, s) = 0 \quad (15)$$

or in Hamiltonian form

$$(\boldsymbol{\alpha} \cdot \mathbf{p} + \beta M + \beta U)\tilde{u}(\mathbf{p}, s) = \epsilon_p \tilde{u}(\mathbf{p}, s) \quad (16)$$

with

$$U = U_S + \gamma^0 U_V \quad (17)$$

where  $U_S$  is an attractive scalar and  $U_V$  the time component of a repulsive vector field. (Notation as in Ref. <sup>47</sup>:  $\beta = \gamma^0$ ,  $\alpha^l = \gamma^0 \gamma^l$ , etc.) The fields,  $U_S$  and  $U_V$ , are in the order of several hundred MeV and strongly density dependent. The solution of Eq. (15) is

$$\tilde{u}(\mathbf{p}, s) = \sqrt{\frac{\tilde{E}_p + \tilde{M}}{2\tilde{M}}} \begin{pmatrix} 1 \\ \frac{\boldsymbol{\sigma} \cdot \mathbf{p}}{\tilde{E}_p + \tilde{M}} \end{pmatrix} \chi_s \quad (18)$$

with

$$\tilde{M} = M + U_S, \quad \tilde{E}_p = \sqrt{\tilde{M}^2 + \mathbf{p}^2}, \quad (19)$$

and  $\chi_s$  a Pauli spinor.

The Brueckner equation now reads

$$\tilde{G}(\tilde{z}) = \tilde{V} + \tilde{V} \frac{Q}{\tilde{z} - h_0} \tilde{G}(\tilde{z}). \quad (20)$$

The essential difference to standard Brueckner theory is the use of the potential  $\tilde{V}$ . As indicated by the tilde, this meson-theoretic potential is evaluated by using the spinors Eq. (18) instead of the free Dirac spinors applied in scattering (and conventional Brueckner theory). Since  $U_S$  (and  $\tilde{M}$ ) are strongly density dependent, so is the potential  $\tilde{V}$ .  $\tilde{M}$  decreases with density. The essential effect in nuclear matter is a suppression of the (attractive)  $\sigma$ -exchange; this suppression increases with density, providing additional saturation. It turns out (see Fig. 7 below) that this effect is so strongly density-dependent that the empirical nuclear matter saturation energy *and* density can be reproduced simultaneously.

The lowest-order energy of nuclear matter is

$$\frac{\mathcal{E}}{A} = \frac{1}{A} \sum_{m \leq k_F} \frac{\tilde{M}}{\tilde{E}_m} \langle m | \boldsymbol{\gamma} \cdot \mathbf{p}_m + M | m \rangle + \frac{1}{2A} \sum_{m, n \leq k_F} \frac{\tilde{M}^2}{\tilde{E}_m \tilde{E}_n} \langle mn | \tilde{G}(\tilde{z}) | mn - nm \rangle - M. \quad (21)$$

The single-particle potential,

$$U(m) = \frac{\tilde{M}}{\tilde{E}_m} \langle m | U | m \rangle = \frac{\tilde{M}}{\tilde{E}_m} \langle m | U_S + \gamma^0 U_V | m \rangle = \frac{\tilde{M}}{\tilde{E}_m} U_S + U_V, \quad (22)$$

is determined from the  $\tilde{G}$ -matrix in formally the usual way,

$$U(m) = Re \sum_{n \leq k_F} \frac{\tilde{M}^2}{\tilde{E}_n \tilde{E}_m} \langle mn | \tilde{G}(\tilde{z}) | mn - nm \rangle \quad (23)$$

with  $m$  below and above the Fermi surface (continuous choice) and

$$\tilde{z} = \epsilon_m + \epsilon_n, \quad (24)$$

where the single particle energy is given by

$$\epsilon_m = \frac{\tilde{M}}{\tilde{E}_m} \langle m | \boldsymbol{\gamma} \cdot \mathbf{p}_m + M | m \rangle + U(m) \quad (25)$$

$$= \tilde{E}_m + U_V. \quad (26)$$

Note that, in this approach, the nucleon states  $|m\rangle$  and  $|n\rangle$  are represented by Dirac spinors of the kind Eq. (18) and an appropriate isospin wavefunction,  $\langle m|$  and  $\langle n|$  are the adjoint Dirac spinors  $\bar{u} = \tilde{u}^\dagger \gamma^0$ ;  $\tilde{E}_m = \sqrt{\tilde{M}^2 + \mathbf{p}_m^2}$ . The normalization of the Dirac spinors is  $\tilde{u}\tilde{u} = 1$ .

Results are shown in Fig. 7 where the lower solid and lower dashed curves repeat the predictions presented in the previous section for the Argonne  $V_{18}$  and the CD-Bonn potentials, respectively. To these curves, we now add the relativistic Dirac effects based upon the formalism just sketched and calculated in Ref. <sup>48</sup>. This results in the upper dashed and solid curves for  $V_{18}$  and CD-Bonn, respectively.

As discussed, this Dirac effect allows a correct reproduction of the saturation density and energy—as demonstrated by the upper CD-Bonn curve. It is also evident that slight overbinding in the nonrelativistic approach is a necessary prerequisite for ultimately predicting density and energy right. As revealed by the upper dashed line in Fig. 7, local potentials lack binding energy and, therefore, cannot reproduce nuclear saturation correctly.

Alternatively, one may take a phenomenological approach in which one tries to simulate the Dirac effect by a repulsive 3NF. This method is pursued by the Urbana group<sup>49</sup> and we have included their results in Fig. 7 in terms of the dotted lines. The lower dotted curve is the variational result with the  $V_{18}$  two-nucleon potential and should be compared with the lower dashed curve (Brueckner with  $V_{18}$ ). The closeness of these two curves confirms what we discussed in conjunction with Fig. 1, namely, a satisfactory agreement between Brueckner theory and the variational approach. The Urbana group developed a repulsive phenomenological 3NF designed to improve the nuclear saturation prediction. Adding this 3NF leads

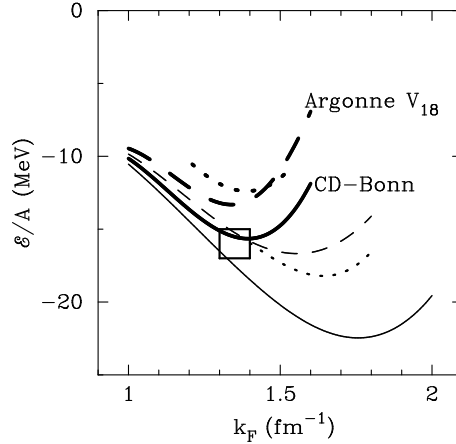


Figure 7. The impact of relativistic Dirac effects on nuclear matter saturation. The lower solid and dashed curves are without and the corresponding upper curves are with Dirac effects. Dashed curves represent Brueckner results based upon the Argonne  $V_{18}$  potential and solid curves correspond to CD-Bonn. Dotted curves are variational results with  $V_{18}$  where the upper dotted curve includes a repulsive 3NF (from Akmal *et al.*<sup>49</sup>).

us from the lower dotted curve to the upper dotted curve. The latter is obviously close to the upper dashed line which implies that the repulsive 3NF is simulating the Dirac effects well. The upper dotted and dashed curves are the final results for Argonne  $V_{18}$  and prove that—no matter what mechanisms are invoked to get the saturation density right—local potentials always underbind nuclear matter.

In conclusion, nonlocality of the nuclear force is crucial to explain nuclear binding quantitatively. This should be no surprise since the nuclear force is inherently nonlocal, anyhow.

## 7 Conclusions

Using Brueckner theory, we have investigated systematically the influence of non-nucleonic degrees of freedom on the predicted properties of nuclear matter.<sup>50</sup> In general, many-body calculations of this kind can be very involved and most cumbersome. However, in the framework of Brueckner theory, these rather sophisticated investigations can be conducted in a straightforward and manageable way. This is one of the great advantages of Brueckner theory.

One result of our investigation is that explicit meson and  $\Delta$ -isobar degrees of freedom do not improve the saturation properties of nuclear matter. However, they teach us something about many-body forces: a mechanism that has the potential of creating many-nucleon forces should be treated consistently in the two- and many-nucleon system. Even though individual contributions caused by this mechanism can be large, the net result turns out to be very small—due to characteristic cancellations between effects from two- and many-nucleon terms. Indeed, the final result is very similar to what is obtained from a *nonlocal* two-nucleon force, since nonlocal-

ity is an inherent quality of the more comprehensive and fundamental fieldtheoretic approach. If the force is local, insufficient binding is predicted.

We also discussed an extension of Brueckner theory in which the relativistic Dirac equation is used for single particle motion (also known as Dirac-Brueckner-Hartree-Fock). This has a substantial impact on nuclear saturation such that the empirical density and energy can be reproduced.

Based upon the work summarized in this talk and the countless papers not mentioned, we conclude that Brueckner theory has contributed in a crucial way to our understanding of the nuclear many-body problem.

### Acknowledgments

This work was supported in part by the U.S. National Science Foundation under Grant No. PHY-9603097.

### References

1. H. Euler, *Z. Physik* **105**, 553 (1937).
2. C. F. von Weizsäcker, *Z. Physik* **96**, 431 (1935).
3. R. Jastrow, *Phys. Rev.* **81**, 165 (1951).
4. K. A. Brueckner *et al.*, *Phys. Rev.* **95**, 217 (1954).
5. K. A. Brueckner, *Phys. Rev.* **96**, 508 (1954); *ibid.* **100**, 36 (1955).
6. K. A. Brueckner and C. A. Levinson, *Phys. Rev.* **97**, 1344 (1955).
7. K. M. Watson, *Phys. Rev.* **89**, 575 (1953).
8. J. Goldstone, *Proc. Roy. Soc. (London)* **A239**, 267 (1957).
9. K. A. Brueckner and J. L. Gammel, *Phys. Rev.* **109**, 1023 (1958).
10. J. L. Gammel and R. M. Thaler, *Phys. Rev.* **107**, 291, 1339 (1957).
11. B. D. Day, *Rev. Mod. Phys.* **39**, 719 (1967).
12. R. Rajaraman and H. A. Bethe, *Rev. Mod. Phys.* **39**, 745 (1967).
13. B. H. Brandow, *Rev. Mod. Phys.* **39**, 771 (1967).
14. H. A. Bethe, *Ann. Rev. Nucl. Sci.* **21**, 93 (1971).
15. P. J. Siemens, *Nucl. Phys.* **A141**, 225 (1970).
16. M. I. Haftel and F. Tabakin, *Nucl. Phys.* **A158**, 1 (1970).
17. F. Coester *et al.*, *Phys. Rev. C* **1**, 769 (1970).
18. D. W. L. Sprung, *Adv. Nucl. Phys.* **5**, 225 (1972).
19. J. W. Clark, *Crisis in Nuclear-Matter Theory*, unpublished (1975); *Nucl. Phys.* **A328**, 587 (1979); *Prog. Part. Nucl. Phys.* **2**, 89 (1979).
20. B. D. Day, *Rev. Mod. Phys.* **50**, 495 (1978).
21. B. D. Day, *Phys. Rev. Lett.* **47**, 226 (1981); *Phys. Rev. C* **24**, 1203 (1981).
22. V. R. Pandharipande and R. B. Wiringa, *Rev. Mod. Phys.* **51**, 821 (1979).
23. S. Fantoni and S. Rosati, *Nuovo Cim.* **25A**, 593 (1975); *ibid.* **43A**, 413 (1978); O. Benhar *et al.*, *Nucl. Phys.* **A328**, 127 (1979).
24. Proc. Int. Conf. on Recent Progress in Many-Body Theories, Trieste, 1978, *Nucl. Phys.* **A328** (1979).
25. R. B. Wiringa and V. R. Pandharipande, *Phys. Lett.* **B99**, 1 (1981); I. E. Lagaris and V. R. Pandharipande, *Nucl. Phys.* **A359**, 349 (1981).

26. B. D. Day and R. B. Wiringa, *Phys. Rev. C* **32**, 1057 (1985).
27. Proc. Fourth Int. Conf. on Recent Progress in Many-Body Theories, San Francisco, 1985, unpublished.
28. R. B. Wiringa *et al.*, *Phys. Rev. C* **29**, 1207 (1984).
29. The single particle potential for a nucleon  $m$  below the Fermi surface is defined in terms of the ‘on-shell’ Brueckner  $G$  matrix by

$$U(m) = Re \sum_{n \leq k_F} \langle mn | G(w) | mn - nm \rangle \quad (27)$$

with starting energy  $w = e_m + e_n$ , where  $e_m$  and  $e_n$  denote the nonrelativistic single particle energies of nucleon  $m$  and  $n$ , respectively. If this same definition is also applied to nucleons above the Fermi surface, we speak of the *continuous choice*. If, however,  $U \equiv 0$  is assumed above  $k_F$ , then we have the *conventional or gap choice*.

30. H. Q. Song, M. Baldo, G. Giansiracusa, and U. Lombardo, *Phys. Rev. Lett.* **81**, 1584 (1998); M. Baldo, private communication.
31. J. P. Jeukenne, A. Lejeune, and C. Mahaux, *Phys. Reports* **25**, 83 (1976).
32. P. Grangé and A. Lejeune, *Nucl. Phys.* **A327**, 335 (1979).
33. C. Mahaux, *Nucl. Phys.* **A328**, 24 (1979).
34. D. Schütte, *Nucl. Phys.* **A221**, 450 (1974).
35. S. S. Schweber, *An Introduction to Relativistic Quantum Field Theory* (Row, Peterson and Co.; Evanston, Ill., U.S.A.; 1961) Chapters 11 and 13.
36. R. Machleidt, K. Holinde, and C. Elster, *Phys. Reports* **149**, 1 (1987).
37. W. H. Dickhoff, A. Faessler, and H. Müther, *Nucl. Phys.* **A389**, 492 (1982).
38. R. Machleidt and K. Holinde, *Phys. Lett.* **152B**, 295 (1985).
39. C. Hajduk, P. U. Sauer, and W. Strueve, *Nucl. Phys.* **A405**, 581 (1983).
40. A. Picklesimer, R. A. Rice, and R. Brandenburg, *Phys. Rev. C* **45**, 2045, 2624 (1992); *ibid.* **46**, 1178 (1992).
41. S. Weinberg, *Phys. Lett.* **B251**, 288 (1990); *Nucl. Phys.* **B363**, 3 (1991); *Phys. Lett.* **B295**, 114 (1992).
42. U. van Kolck, *Phys. Rev. C* **49**, 2932 (1994).
43. V. G. J. Stoks *et al.*, *Phys. Rev. C* **49**, 2950 (1994).
44. R. B. Wiringa, V. G. J. Stoks, and R. Schiavilla, *Phys. Rev. C* **51**, 38 (1995).
45. R. Machleidt, F. Sammarruca, and Y. Song, *Phys. Rev. C* **53**, 1483 (1996).
46. We note that the very close agreement between the CD-Bonn curve (thin solid line) and the thick solid curve in Fig. 6 is, of course, accidental. However, the agreement within  $\pm 1$  MeV is not.
47. J. D. Bjorken and S. D. Drell, *Relativistic Quantum Mechanics*, McGraw-Hill, New York (1964).
48. R. Brockmann and R. Machleidt, *Phys. Rev. C* **42**, 1965 (1990).
49. A. Akmal *et al.*, *Phys. Rev. C* **58**, 1804 (1998).
50. A comprehensive and more detailed review of the topics discussed in this talk and the pertinent literature can be found in sections 9 and 10 of Ref. <sup>51</sup> which is also the original reference for many of the results presented.
51. R. Machleidt, *Adv. Nucl. Phys.* **19**, 189 (1989).